# CHAPTER 6

## *On the control of magnetic anisotropy through*

## *an external electric field*

**Abstract**

The effect of an external electric field on the magnetic anisotropy of a single-molecule magnet has been investigated, with the help of DFT. The magnetic anisotropy of a pseudo-octahedral Co(II) complex namely, $[Co^{II}(dmphen)_2(NCS)_2]$, has been investigated in the present chapter in connection to the tunability of the magnetic anisotropy through external electric field. The application of an electric field can alter the magnetic anisotropy from "easy-plane" ($D>0$) to "easy-axis" ($D<0$) type. The alteration in the magnetic anisotropy is found due to the change in the Rashba spin-orbit coupling by the external electric field. This variation in the Rashba spin-orbit coupling is further confirmed by the generation of the spin dependent force in the molecule which is later found to manifest separation of $\alpha$- and $\beta$- spins in opposite ends of the molecule. The excitation analysis performed through time-dependent DFT also predicts that the external electric field facilitates metal to $\pi$-acceptor ligand charge transfer, leading to uniaxial magnetic anisotropy and concomitant spin Hall effect in a single molecule.

## 6.1. Introduction

Magnetic anisotropy is of central importance in the understanding of single-molecule magnets (SMM).[1] Molecules that exhibit slow relaxation of their magnetization, leading to a magnetic hysteresis at low temperatures, are termed as SMMs.[2] The genesis of this interesting magnetic property in a molecule is the existence of two ground states of magnetization $+M_S$ and $-M_S$ separated by an energy barrier. This bistability of the SMMs makes them indispensable in the domain of data storage[3] and quantum computing.[4] SMMs are often characterized by a large easy-axis-type magnetic anisotropy and concomitant high energy barrier ($U$), which restricts the reversal of the magnetization from $+M_S$ to $-M_S$. To reorient spin in the magnetic molecules, the barrier $U$ can be given by $|D|S^2$ for molecules with integer spins and $|D|\left(S^2 - \frac{1}{4}\right)$ for molecules with half integer spins. $D$ is the zero-field splitting (ZFS) parameter and $S$ is the ground-state spin. The large negative ZFS parameter ($D$) causes the spin ($S$) of the molecule to point along a preferred easy-axis and makes it a nanomagnet. The requirement of proper SMMs for apposite needs prompted researchers to study the tuning of magnetic anisotropy.

The most investigated molecule of this type is [$Mn_{12}O_{12}$-$(CH_3COO)_{16}(H_2O)_4$], which is popularly known as $Mn_{12}$-ac.[5] A central tetrahedron of four $Mn^{4+}$ ions ($S=3/2$) and eight surrounding $Mn^{3+}$ ($S=2$) ions construct the magnetic core of $Mn_{12}$-ac. This compound, which was first synthesized by Lis,[6] has drawn the attention of the scientific community because it has a strikingly large molecular magnetic moment,[7] and magnetic bistability with a high magnetization reversal barrier.[8] It is evident from the above discussion that the spin-reversal barrier is dependent on the total spin, $S$, and the ZFS parameter, $D$. The most convenient way to increase the energy barrier within a SMM is through the ground-state spin $S$. However, increasing $S$ leads to an effective reduction in the ZFS parameter, $D$,[9] which results in a net decrease in the spin-reorientation barrier, $U$. Thus, the only way to control $U$ is through modulation of the ZFS parameter, $D$. Although a plethora of compounds with properties that resemble those of $Mn_{12}$-ac have been synthesized to date,[10] the rational design of SMMs with tunable $S$ and $D$ is far from being achieved. Thus, modulation of the ZFS parameter is now a promising field of research for its wide-ranging applications in high-density information storage, quantum computing, and spintronic devices.[11]

Cobalt(II) complexes are known to exhibit strong spin–orbit coupling in comparison to manganese(II–IV), iron(III), or nickel(-II), to which the distinguished members of the SMM family belong.[12] This is because such octahedral or pseudo-octahedral cobalt(II) ions are known to exert strong first-order orbital magnetism. The ground-state spin configuration for Co(II) in an octahedral coordination environment is $t_{2g}^5 e_g^2$, which designates a $^4F$ ground state.[13] The $^4F$ ground state is split into two triplet states ($^4T_{1g}$, $^4T_{2g}$) and one singlet state ($^4A_{2g}$). The triplet nature of the $^4T_{1g}$ ground state is responsible for first-order orbital momentum.[13] The large unquenched orbital angular momentum in $Co^{II}$ makes it an important candidate for the study of magnetic anisotropy. Current literature in the domain of SMM research suggests a drift towards the tuning of the magnetic anisotropy through various means.

The modulation of the ZFS parameter by ligand substitution has recently been studied in the framework of DFT.[14] Structural modification in an octahedral $Cr^{III}$ system can switch the magnetization behavior of a molecule from easy-plane to easy-axis type. Herein, we investigate the effect of an external electric field on the ZFS parameter of a pseudo-octahedral $[Co^{II}-(dmphen)_2(NCS)_2]$ complex (dmphen=2,9-dimethyl-1,10-phenanthroline; Figure 6.1) to control magnetization through external stimuli. The use of an electric field in tuning magnetic and transport properties has also been demonstrated recently.[15] To control magnetization, the use of an electric field is highly advantageous.[16] Although the bulk properties of SMMs are well documented in their unperturbed state,[17] the study of the effect of an external electric field on the magnetization of SMMs is relatively recent.[18]
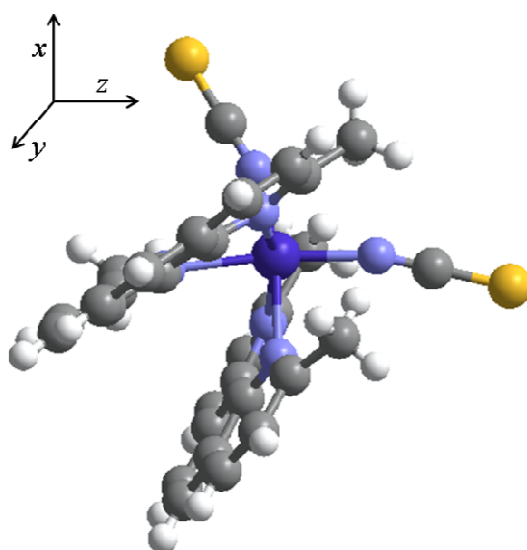


**Figure 6.1.** Structure of the pseudo-octahedral $Co^{II}$-complex, $[Co^{II}(dmphen)_2(NCS)_2]$ .

## 6.2. Theoretical Background and Method

The formation of a static electric field between two oppositely charged parallel plates is well known from the laws of classical electrophysics. It is also common practice to create a uniform static field between the central area of large parallel plates because in that area the electric lines of force become parallel. This simple concept from elementary physics encouraged us to construct a device to calculate ZFS under the influence of an external electric field. Thus, to realize the magnetization behavior of the molecule under an electric pulse, we placed the molecule between two oppositely charged parallel plates with an area of about 600 $Å^2$. We chose the atomic arrangements of the Pt (111) surface, and subsequently, replaced the atoms with point charges uniformly to create the charged plates. The plates were 40 Å apart, which maintained a distance of at least 18 Å from the molecule and would avoid any structural deformation due to point charges. The whole arrangement is pictorially represented in Figure 6.2. This is typically the same arrangement as a parallel-plate capacitor.

The left plate is charged as positive, while the right plate contains negative point charges of the same magnitude in the platinum atomic positions. In this way, we create an electric field along the positive $z$-axis. Calculations of the ZFS parameters were performed by following the methodology discussed in the following paragraphs.
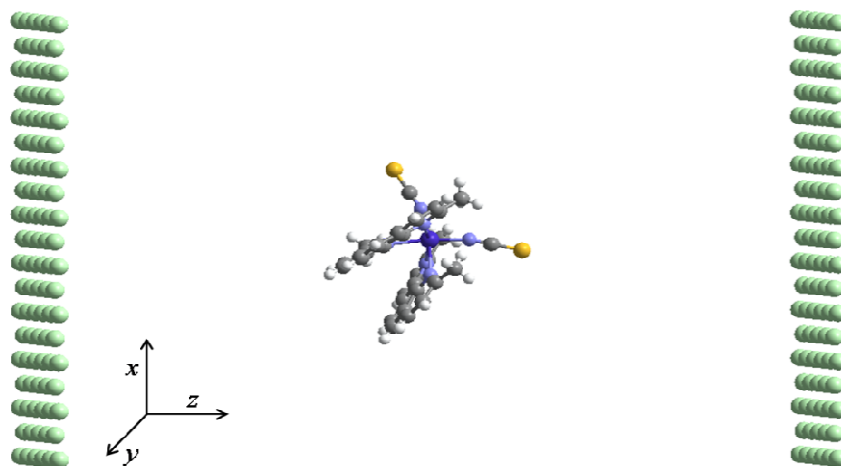


**Figure 6.2.** The arrangement of $[Co^{II}(dmphen)_2(NCS)_2]$ complex between two oppositely charged parallel plates.

ZFS lifts the degeneracy of the $M_S$ states in a molecule with $S>1/2$, in the absence of an external magnetic field. It is customary to treat the spin–orbit coupling contribution to ZFS through an uncoupled perturbation theoretical approach in unrestricted Kohn–Sham formalism.[19] The corresponding correction to the total energy can be expressed as eqn (6.1):[20]

$$\Delta_2 = \sum_{\sigma\sigma'} \sum_{ij} M_{ij}^{\sigma\sigma'} S_i^{\sigma\sigma'} S_j^{\sigma'\sigma} ,$$

(6.1)

in which $S_i^{\sigma\sigma'} = \left\langle \chi^\sigma \,/\, S_i \,/\, \chi^{\sigma'} \right\rangle$; $\chi^\sigma$ and $\chi^{\sigma'}$ are different spinors; $\sigma$ denotes different spin degrees of freedom and the coordinate labels, $x$, $y$, and $z$ are represented by $i$, $j$, and so forth. The matrix elements $M_{ij}^{\sigma\sigma'}$ in eqn (6.1) are described by eqn (6.2)

$$M_{ij}^{\sigma\sigma'} = -\sum_{kl} \frac{\left\langle \varphi_{l\sigma} \,/\, V_i \,/\, \varphi_{k\sigma'} \right\rangle \left\langle \varphi_{k\sigma'} \,/\, V_j \,/\, \varphi_{l\sigma} \right\rangle}{\varepsilon_{l\sigma} - \varepsilon_{k\sigma'}} .$$

(6.2)

In this equation $\varepsilon_{l\sigma}$ and $\varepsilon_{k\sigma'}$ are energies of the occupied, $\varphi_{l\sigma}$, and unoccupied, $\varphi_{k\sigma'}$, states, respectively. In the absence of a magnetic field, the change in energy of the system in the second-order is written as eqn (6.3):

$$\Delta_2 = \sum_{ij} \gamma_{ij} \left\langle S_i \right\rangle \left\langle S_j \right\rangle .$$

(6.3)

Upon diagonalization of the anisotropy tensor, $\gamma$, the eigenvalues $\gamma_{xx}$, $\gamma_{yy}$, and $\gamma_{zz}$ are obtained and the second-order perturbation energy can now be written as eqn (6.4)

$$\Delta_2 = \frac{1}{3}\left(\gamma_{XX} + \gamma_{YY} + \gamma_{ZZ}\right)S(S+1)$$
$$+ \frac{1}{3}\left[\gamma_{ZZ} - \frac{1}{2}\left(\gamma_{XX} + \gamma_{YY}\right)\right]\left[3S_Z^2 - S(S+1)\right] \quad (6.4)$$
$$+ \frac{1}{2}\left(\gamma_{XX} - \gamma_{YY}\right)\left(S_X^2 - S_Y^2\right)$$

These anisotropy tensor components ($\gamma_{xx}$, $\gamma_{yy}$, $\gamma_{zz}$) are parameterized to obtain eqn (6.5) as a simplified expression:

$$H_{ZFS} = D[S_z^2 - \frac{1}{3}S(S+1)] + E[S_x^2 - S_y^2] \quad (6.5)$$

in which $D$ and $E$ are axial and rhombic ZFS parameters, respectively. Calculation of parameters $D$ and $E$ was performed in the ORCA suit of a density functional package.[21] The methodology adopted herein was the BPW91 functional,[22] TZV basis set,[23] with the auxiliary TZV/J Coulomb-fitting basis set.[24] This methodology, under unrestricted Kohn--Sham formalism, as adopted herein, is being widely used to compute ZFS parameters.[22a,25] Although there are several methods available for the computation of the ZFS parameter, the Pederson and Khanna (PK) method is known to produce the correct sign of the ZFS parameter;[22a,26] therefore, we use this methodology[20] to calculate the ZFS parameters. The ZFS contributions predicted by this method show fair agreement with accurate ab initio and experimental results.


## 6.3. Results and Discussions

Single-point calculations on the crystallographic structure, which are available in ref.28, were performed and used for further calculations. It is known from the EPR spectra of complex [Co$^{II}$(dmphen)$_2$(NCS)$_2$] that it has ground-state spin $S$=3/2. The value of $D$ is calculated for the complex in its unperturbed ground state and also under the application of bias voltage in the range of $-4\times10^{-3}$ to $4\times10^{-3}$a.u. Herein, the positive and negative values of the external electric field are designated with the application of the field along the positive direction of the $z$ axis, that is, along one axial direction of the Co-NCS bond. The complex is put under a static electric field of different strengths, according to the arrangement discussed in the previous section. It was shown previously that typically a critical electric field in the order of 0.01a.u. was required to bring about ionization in a molecule.[27] Hence, application of an electric field in the order of 0.004a.u., as in the present case, is not expected to bring about any undesired polarization or ionization of the molecule.

In the ground state, the ZFS parameter of the complex is positive, which signifies easy-plane type magnetic anisotropy. The computed value of $D$ is given in Table 6.1, along with individual excitation contributions. The MAE barrier, $U$, was also computed and compared with experimental values.[28] We found reasonable agreement of the calculated value of $U$ with the experimentally obtained MAE barrier. However, from experimental results reported previously,[28] we also find an ab initio CASSCF result of $D = +196$ cm$^{-1}$ with a clear dictation of the disagreement between the calculated and experimental values of $U$. There has been a debate about whether DFT is better than ab initio methods in the logical prediction of ZFS parameters. Nevertheless, in a recent study, it was categorically shown that DFT provided efficient estimates of the ZFS parameters compared with popular ab initio methods.[29]

**Table 6.1.** A comparison of the experimental magnetic anisotropy energy (MAE) barrier with that computed at the BPW91/TZV level and the individual excitation contributions towards the ZFS parameter in the ground state.

| Computed ZFS parameter $D$ and $U$ at BPW91/TZV level | | | Experimental[28] MAE barrier in cm$^{-1}$ |
|---|---|---|---|
| Individual excitation contributions to ZFS | | Calculated ZFS Parameter $D$ in cm$^{-1}$ | Calculated MAE barrier in cm$^{-1}$ | |
| $\alpha \rightarrow \alpha$ | 0.178 | | | |
| $\alpha \rightarrow \beta$ | 1.385 | | | |
| $\beta \rightarrow \alpha$ | –0.266 | 6.561 | 13.122 | ~17 |
| $\beta \rightarrow \beta$ | 5.265 | | | |

Computation of the ZFS parameters is also executed under different external electric fields. The values of $D$, along with the individual excitation contributions towards ZFS, are given in Table 6.2. A plot of the variation in $D$ with applied electric field in Figure 6.3 suggests that after certain critical field strength the easy-plane magnetization of the Co$^{II}$ complex changes to easy-axis type. Thus, it can be interpreted that, after a threshold field, the molecule starts to behave as an SMM. Moreover, the switch in the $D$ value in both field directions is also clear from Figure 6.3. This flip in $D$ is in the range of $1.6\times10^{-3}$ and $1.7\times10^{-3}$ a.u of electric field strength when the field is applied along the positive $z$ axis.
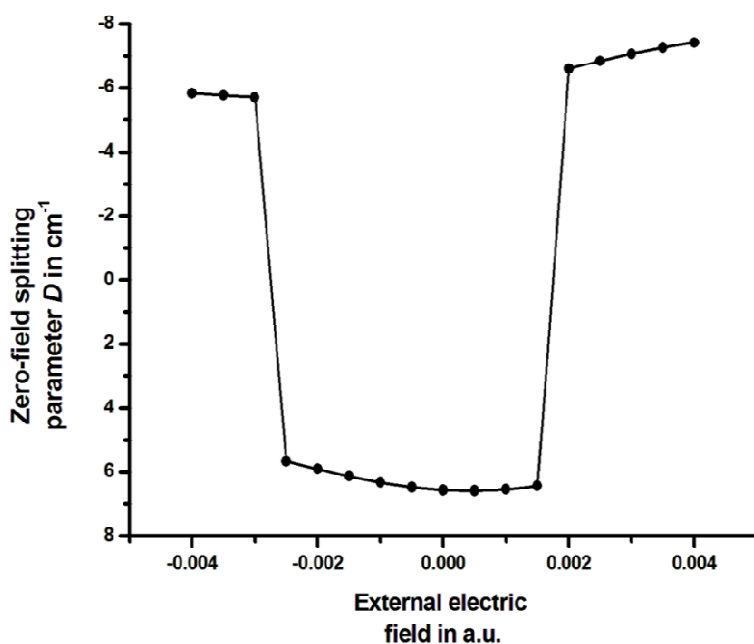
**Figure 6.3.** A plot of the variation in $D$ with external electric field.

**Table 6.2.** The ZFS parameters computed at the BPW91/TZV level and the individual excitation contributions towards ZFS under the influence of a finite electric field.

| External Electric Field (in a.u.) | ZFS parameter $D$ (in cm$^{-1}$) | Different Excitation Contributions to $D$ | | | |
|:---:|:---:|:---:|:---:|:---:|:---:|
| | | $\alpha \rightarrow \alpha$ | $\alpha \rightarrow \beta$ | $\beta \rightarrow \alpha$ | $\beta \rightarrow \beta$ |
| Under negative applied field | | | | | |
| −0.0040 | −5.828 | −0.132 | −1.288 | 0.211 | −4.619 |
| −0.0035 | −5.762 | −0.131 | −1.267 | 0.216 | −4.580 |
| −0.0030 | −5.700 | −0.130 | −1.236 | 0.222 | −4.557 |
| −0.0025 | 5.668 | 0.168 | 1.429 | −0.230 | 4.301 |
| −0.0020 | 5.909 | 0.172 | 1.451 | −0.238 | 4.524 |
| −0.0015 | 6.133 | 0.175 | 1.463 | −0.247 | 4.742 |
| −0.0010 | 6.325 | 0.177 | 1.460 | −0.255 | 4.943 |
| −0.0005 | 6.470 | 0.178 | 1.436 | −0.261 | 5.117 |
| Under positive applied field | | | | | |
| 0.0005 | 6.578 | 0.177 | 1.323 | −0.268 | 5.347 |
| 0.0010 | 6.537 | 0.177 | 1.231 | −0.270 | 5.399 |
| 0.0015 | 6.428 | 0.179 | 1.105 | −0.273 | 5.418 |
| 0.0020 | −6.593 | −0.107 | −0.646 | 0.258 | −6.096 |
| 0.0025 | −6.835 | −0.107 | −0.602 | 0.255 | −6.380 |
| 0.0030 | −7.059 | −0.104 | −0.560 | 0.249 | −6.644 |
| 0.0035 | −7.254 | −0.107 | −0.516 | 0.248 | −6.879 |
| 0.0040 | −7.406 | −0.110 | −0.477 | 0.246 | −7.066 |

It can be seen from Tables 6.1 and 6.2 that the major excitation contribution towards *D* comes from the *β→β* excitation. To further investigate the effect of electric field on the excitation pattern of the molecule, we performed time-dependent (TD) DFT calculations at the same computational level by using the Gaussian09W[30] suite of programs. Excitations with maximum oscillator strengths are characterized to involve *β* electrons only. The molecular orbitals (MOs) from and to which excitation occurs are summarized in Table 6.3. In the ground state, the source MO involves the metal *d* orbitals and the thiocyanate ligands. The destination MOs in the unperturbed state corroborate the interaction of the dmphen ligand with the central metal ion. No significant change in the picture is observed for a field strength lower than that of the critical value at which *D* is still positive. On the other hand, above the critical field strength, the excitation spectrum reverses. At a field strength of 0.004 a.u., the source MO is essentially centered on the dmphen ligand, whereas the destination is the MO based on the NCS ligands. Hence, from the above discussion, it is evident that the natural tendency of the electrons to flow towards the *π*-acceptor NCS ligands is developed at a field strength higher than that of the critical field. It follows from our previous work that the *π*-accepting tendency of the ligands exerts easy-axis-type magnetic anisotropy (*D*<0) in a molecule.[14] Thus, it can be concluded that the switch in the *D* value arises from metal-to-ligand back charge transfer in the molecule facilitated by exposure to the external electric field.
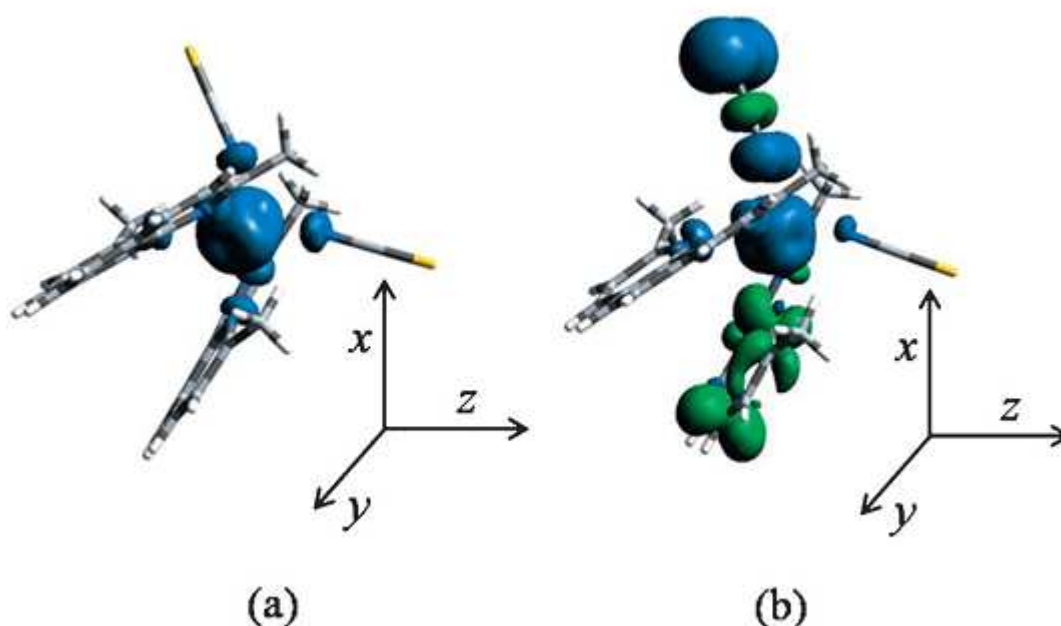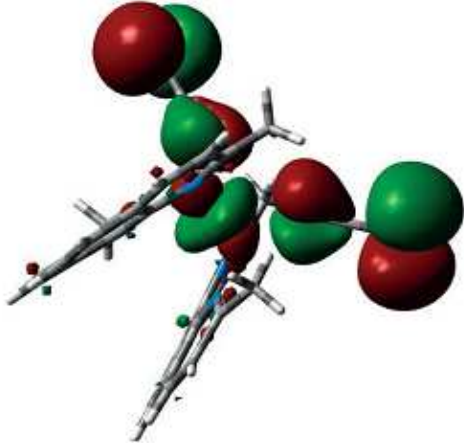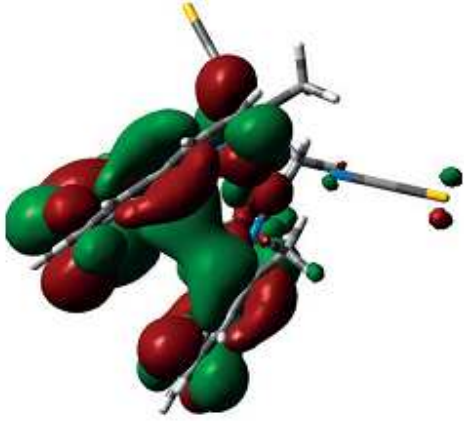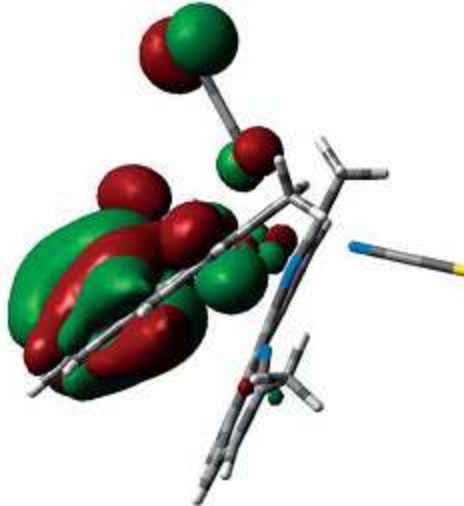


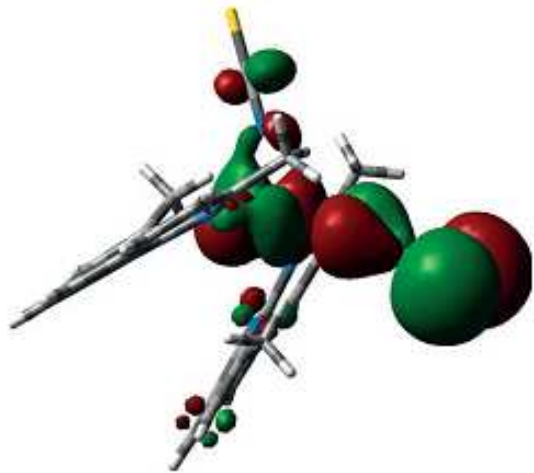(a)                                    (b)

**Figure 6.4.** The spin-density plots (at an isosurface value of 0.004) of the Co(II) complex in a) the ground state and b) under the applied electric field with a magnitude of 4.0×103 a.u. The blue color specifies *α*-spin density and the green color indicates *β*-spin density.

**Table 6.3.** The excitation behavior of [CoII(dmphen)2(NCS)2] in the ground state and under application of a finite electric field computed at the BPW91/TZV level.

| Applied electric field strength [a.u.] | Source MO | Destination MO |
|---|---|---|
| 0.000 |  |  |
| | 136 $\beta$ | 138 $\beta$ |
| 0.004 |  |  |
| | 134 $\beta$ | 137 $\beta$ |

A similar and more interesting portrayal of the phenomenon is found in the spin density plots depicted in Figure 6.4. We compared the spin densities of the complex at zero-external field and finite external electric fields above the critical field. Separation of the $\alpha$ and $\beta$ spins is observed at a higher electric field strength than that of the unperturbed state. This dispersion of the $\beta$ spin is further confirmed from a comparison of the density of states (DOS)

plots at different electric fields given in Figure D.S1 in the Supporting Information. Close inspection of the DOS plots reveals the shift in the energies of the $\alpha$ and $\beta$ electrons. Although electrons of both spins show a shift in the energy level, an alteration in the energy of the $\beta$ spin is specifically observed. This interesting feature of a shift in the energy levels of different spins due to opposite spin accumulation on two different sides of a molecule is termed as the spin Hall effect.[31]

The molecular origin of this correlation of the electron spin and applied electric field is steered by spin-orbit coupling. In this context, the Rashba-type spin-orbit interaction draws the attention of the scientific community due to its tunable nature under an applied electric field.[32] The spin-orbit coupling Hamiltonian in eqn (6.6) describes the coupling of electron spin $\sigma$ and momentum $p$ under an external electric field $E$:

$$\hat{H}_{SO} = -\mu_B \sigma \left( p \frac{E}{2mc^2} \right) \qquad (6.6)$$

in which $\sigma$, $\mu_B$, and $c$ are Pauli spin matrices, the Bohr magneton, and the velocity of light, respectively. It is evident from eqn (6.6) that a momentum-dependent internal magnetic field is generated, as shown in eqn (6.7):

$$B_{int} = p \frac{E}{2mc^2} \qquad (6.7)$$

and the resulting spin polarization is crucially dependent on both $p$ and $E$ and their relative directions.[33] It can be argued that there is a generalized tendency of the electrons to move towards the $\pi$-accepting NCS ligands, and hence, the direction of the resultant momentum of the electrons can be along the $+x$ axis (see Appendix D). The interaction of the electron momentum with the external electric field generates an internal magnetic field. A magnetic field thus generated, in turn, accelerates the $\alpha$ and $\beta$ electrons in opposite directions through a spin-dependent force, represented by eqn(6.8)

$$F_{\uparrow\downarrow} = \pm g\mu_B \frac{dB_{int}}{dq} \qquad (6.8)$$

in which $g$ is the electronic $g$ factor and $\mu_B$ is the Bohr magneton. The clear bifurcation of the $\alpha$ and $\beta$ spin densities in opposite directions in the present complex indicates a modification in the spin-orbit interaction. It is also commonly understood that the ZFS in metal systems originates from spin-orbit coupling. Thus, modification in the spin-orbit coupling is further established through alteration to the ZFS parameter under an external electric field.

## 6.4. Conclusion

Emerging interest in mononuclear complexes, in comparison to polynuclear ones, has meant that the field of quantum magnets has turned to tuning of the ZFS parameter $D$ through structural modification or external aids. This study contemplated the magnetic anisotropy of

an octahedral $Co^{II}$ complex, namely, $[Co^{II}(dmphen)_2(NCS)_2]$, in connection with the tunability of ZFS parameter $D$ by exploiting an electric field as an external stimuli. Previously, it was shown that the presence of a $\pi$-accepting ligand in the axial position of an octahedral complex could result in magnetization of the molecular magnetic dipole along a specific direction. The external electric field in the present situation assisted such metal-to-ligand charge transfer and led to a switchover in the anisotropic characteristics. A spin-Hall spatial spin separation was also observed due to modulation in the Rashba spin-orbit coupling in a single molecule, for the first time, rather than in mesoscopic systems.

## 6.5. References

**1.** (a) Boussac, A.; Girerd, J. J.; Rutherford, A. W. *Biochemistry* **1996**, *35*, 6984; (b) Horner, O.; Rivire, E.; Blondin, G.; Un, S.; Rutherford, A. W.; Girerd, J. J.;  Boussac, A. *J. Am. Chem. Soc.* **1998**, *120*, 7924 – 7928; (c) Dub, C. E.; Sessoli, R.; Hendrich, M. P.; Gatteschi, D.; Armstrong, W. H. *J. Am. Chem. Soc.* **1999**, *121*, 3537 – 3538; (d) Wernsdorfer, W.; Sessoli, R. *Science* **1999**, *284*, 133.

**2.** (a) Sessoli, R.; Tsai, H. L.; Schake, A. R.; Wang, S. Y.; Vincent, J. B.; Folting, K.; Gatteschi, D.; Christou, G.; Hendrickson, D. N. *J. Am. Chem. Soc.* **1993**, *115*, 1804 – 1816; (b) Gatteschi, D.; Sessoli, R.; Villain, J. In *Molecular Nanomagnets,* Oxford University Press, New York, **2006**; (c) Milios, C. J.; Vinslava, A.; Wernsdorfer, W.; Moggach, S.; Parsons, S.; Perlepes, S. P.; Christou, G.; Brechin, E. K. *J. Am. Chem. Soc.* **2007**, *129*, 2754 – 2755; (d) Yoshihara, D.; Karasawa, S.; Koga, N. *J. Am. Chem. Soc.* **2008**, *130*, 10460 – 10461.

**3.** Mannini, M.; Pineider, F.; Sainctavit, P.; Danieli, C.; Otero, E.; Sciancalepore, C.; Talarico, M.; Arrio, M. A.; Cornia, A.; Gatteschi, D.; Sessoli, R. *Nat. Mater.* **2009**,*8*, 194 – 197.

**4.** (a) Leuenberger, M. N.; Loss, D.; *Nature* **2001**, *410*, 789 – 793; (b) Ardavan, A.; Rival, O.; Morton, J. J. L.;  Blundell, S. J.; Tyryshkin, A. M.; Timco, G. A.; Winpenny, R. E. P.; Phys. Rev. Lett. **2007**, *98*, 057201; (c) Stamp, P. C. E.; Gaita-Arino, A. J. *Mater. Chem.* **2009**, *19*, 1718 – 1730.

**5.** Sessoli, R., Gatteschi, D.; Caneschi, A.; Novak, M. A. *Nature* **1993**, *365*, 141 – 143.

**6.** Lis, T. *ActaCryst. B* **1980**, *36*, 2042 – 2046.

**7.** Caneschi, A.; Gatteschi, D.; Sessoli, R.; Barra, A. L.; Brunel, L. C.; Guillot, M. *J. Am. Chem. Soc.* **1991**, *113*, 5873 – 5874.

**8.** Lawrence, J.; Lee, S. C.; Kim, S.; Anderson, N.; Hill, S.; Murugesu, M.; Christou, G. *AIP Conf. Proc.* **2006**, *850*, 1133 – 1134.

**9.** (a) Waldmann, O. *Inorg. Chem.* **2007**, *46*, 10035 – 10037; (b) Kirchner, N.; van Slageren, J.; Dressel, M. *Inorg. Chim. Acta.* **2007**, *360*, 3813 – 3819.

**10.** Arom, G.; Brechin, E. K. *Struct. Bonding (Berlin)* **2006**, *122,* 1 – 67.

**11.** (a) Bogani, L.; Wernsdorfer, W. *Nat. Mater.* **2008**, *7*, 179 – 186; (b) Urdampilleta, M.; Klyatskaya, S.; Cleuziou, J.P.; Ruben, M.; Wernsdorfer, W.; *Nat. Mater.* **2011**, *10*, 502 – 506; c) Ritter, S. K. *Chem. Eng. News* **2004**, *82*, 29–32.

**12.** Liu, J.; Datta, S.; Bolin, E.; Lawrence, J.; Beedle, C. C.; Yang, E. C.; Goy, P.; Hendrickson, D. N.; Hill, S.; *Polyhedron* **2 009**, *28*, 1922 – 1926.

**13.** (a) Lloret, F.; Julve, M.; Cano, J.; Ruiz-Garca, R.; Pardo, E. *Inorg. Chim. Acta* **2008**, *361*, 3432 – 3445; (b) Palii, A.; Tsukerblat, B.; Clemente-Juan, J. M.; Coronado, E.; *Int. Rev. Phys. Chem.* **2010**, *29*, 135 – 230.

**14.** Goswami, T.; Misra, A. *J. Phys. Chem. A* **2012**, *116*, 5207 – 5215.

**15.** Shil, S.; Misra, A.; *RSC Adv*. **2013**, *3*, 14352 – 14362.

**16.** (a) Chiba, D.; Sawicki, M.; Nishitani, Y.; Nakatani, Y.; Matsukura, F.; Ohno, H. *Nature* **2008**, *455*, 515 – 518; (b) Lebeugle, D.; Mougin, A.; Viret, M.; Colson, D.; Ranno, L. *Phys. Rev. Lett.* **2009**, *103*, 257601.

**17.** (a) Accorsi, S.; Barra, A. L.; Caneschi, A.; Chastanet, G.; Cornia, A.; Fabretti, A. C.; Gatteschi, D.; Mortalo, C.; Olivieri, E.; Parenti, F.; Rosa, P.; Sessoli, R.; Sorace, L.; Wernsdorfer, W.; Zobbi, L. *J. Am. Chem. Soc.* **2006**, *128*, 4742 –4755; (b) Gregoli, L.; Danieli, C.; Barra, A. L.; Neugebauer, P.; Pellegrino, G.; Poneti, G.; Sessoli, R.; Cornia, A.; *Chem. Eur. J.* **2009**, *15*, 6456 – 6467.

**18.** Zyazin, A. S.; van den Berg, J. W. G.; Osorio, E. A.; van der Zant, H. S. J.; Konstantinidis, N. P.; Leijnse, M.; Wegewijs, M. R.; May, F.; Hofstetter, W.; Danieli, C.; Cornia, A. *Nano Lett.* **2010**, *10*, 3307 – 3311.

**19.** Zein, S.; Duboc, C.; Lubitz, W.; Neese, F. *Inorg. Chem.* **2008**, *47*, 134.

**20.** Pederson, M. R.; Khanna, S. N. *Phys. Rev.B* **1999**, *60*, 9566 – 9572.

**21.** Neese, F. *ORCA 2.8.0; University of Bonn, Bonn, Germany,* **2010**.

**22.** (a) van Wllen, C. *J. Chem. Phys.* **2009**, *130*, 194109; (b) Aquino, F.; Rodriguez, J. H. *J. Phys. Chem. A* **2009**, *113*, 9150 – 9156.

**23.** (a) Schfer, A.; Horn, H.; Ahlrichs, R. *J. Chem. Phys.* **1992**, *97*, 2571 – 2577; (b) Schfer, A.; Huber, C.; Ahlrichs, R. *J. Chem. Phys.* **1994**, *100*, 5829 –5835.

**24.** Weigend, F. *Phys. Chem. Chem. Phys.* **2006**, *8*, 1057 – 1065.

**25.** (a) Park, K.; Pederson, M. R.; Richardson, S. L.; Aliaga-Alcalde, N.; Christou, G. *Phys. Rev. B* **2003**, *68*, 020405; (b) Ribas-AriÇo, J.; Baruah, T.; Pederson, M. R. *J. Am. Chem. Soc.* **2006**, *128*, 9497 – 9505.

**26.** Aquino, F.; Rodriguez, J. H. *J. Chem. Phys.* **2005**, *123*, 204902.

**27.** (a) Davari, N.; P.-O. strand, Ingebrigtsen, S.; Unge, M. *J. Appl. Phys.* **2013**, *113*, 143707; (b) Davari, N.; P.-O. strand, Van Voorhis, T.; *Mol. Phys.* **2013**, *111*, 1456 – 1461; (c) Smirnov, M. B.; Krainov, V. P. *J. Exp. Theor. Phys.* **1997**, *85*, 447 – 450.

**28.** Vallejo, J.; Castro, I.; Ruiz-Garca, R.; Cano, J.; Julve, M.; Lloret, F.; Munno, G. D.; Wernsdorfer, W.; Pardo, E. *J. Am. Chem. Soc.* **2012**, *134*, 15704 –15707.

**29.** Singh, S. K.; Rajaraman, G. *Chem. Eur. J.* **2013**, *19*, 1 – 12.

**30.** Frisch, M. J.; Trucks, G. W.; Schlegal, H. B.; Scuseria, G. E.; Robb, M. A.; Cheesman, J. R.; Zakrzewski, V. G.; Montgomerg, J. A.; Strtmann, R. E.; Burant, J. C.; Dapprich, S.; Milliam, J. M.; Daniels, A. D.; Kudin, K. N.; Strain, M. C.; Farkas, O.; Tomasi, J.; Barone, V.; Cossi, M.; Camme, R.; Mennucci, B.; Pomelli, C.; Adamo, C.; Clifford, S.; Ochterski, J.; Petersson, G. A.; Ayala, P. Y.; Cui, Q.; Morokuma, K.; Rega, N.; Salvador, P.; Dannenberg, J. J.; Malich, D. K.; Rabuck, A. D.; Raghavachari, K.; Foresman, J. B.; Cioslowski, J.; Ortiz, J. V.; Baboul, A. G.; Stetanov, B. B.; Liu, G.; Liashenko, A.; Piskorz, P.; Komaromi, I.; Gomperts, R.; Martin, R. L.; Fox, D. J.; Keith, T.; Al-Laham, M. A.; Peng, C. Y.; Nsnsyskkara, A.; Challacombe, M.; Gill, P. M. W.; Johnson, B.; Chen, W.; Wong, M. W.; Andres, J. L.; Gonzalez, C.; Head-Gordon, M.; Replogle E. S.; Pople, J. A. GAUSSIAN09, Revision A.02, Gaussian Inc., Pittsburgh (2009).

**31.** Beeler, M. C.; Williams, R. A.; Jimenez-Garcia, K.; LeBlanc, L. J.; Perry, A. R.; Spielman, I. B. *Nature* **2013**, *498*, 201 – 204.

**32.** Nitta, J.; Akazaki, T.; Takayanagi, H.; Enoki, T.; *Phys. Rev. Lett.* **1997**, *78*, 1335.

**33.** Dresselhaus, G. *Phys. Rev.* **1955**, *100*, 580 – 586.